

Electronic resonances in expanding non-neutral ultracold plasma

S. Ya. Bronin,¹ E. V. Vikhrov,¹ S. A. Saakyan,^{1,2} B. B. Zelener,¹ and B. V. Zelener^{1,*}

¹*Joint Institute for High Temperatures of the Russian Academy of Sciences,
Izhorskaya St. 13, Bldg. 2, Moscow 125412, Russia*

²*National Research University Higher School of Economics (NRU HSE), Myasnitskaya St. 20, Moscow 101000, Russia*

(Dated: November 27, 2023)

We present a calculation of the natural oscillation spectrum of inhomogeneous non-neutral ultracold plasma. The collective modes of these plasma oscillations are recorded in experiments as absorption resonances of radio-frequency electric field. It is shown that in the presence of friction of the electronic component, a discrete spectrum of plasma eigenoscillations is formed. Dependence of the frequency of these resonances on the charge imbalance and on the expansion time is obtained. Good agreement with the experiments of different authors is noted.

I. INTRODUCTION

Experimental study of ultracold plasma (UCP) makes it possible to find the basic physical mechanisms of the processes occurring in any fully ionized plasma, both in case of stationary conditions and during plasma expansion. This is due to the well-controlled initial conditions and relatively slow expansion dynamics. In addition, only the Coulomb interaction between particles is essential in the UCP, while other interactions can be neglected. At present, a fairly large amount of experimental data have been obtained for the UCP of various chemical elements (Xe, Sr, Rb, Ca) with various densities, various numbers of particles, and various initial temperatures of electrons and ions. Many theoretical papers devoted to this field have also been published (see reviews [1, 2]). Most of the experimental results for the UCP are associated with the study of ions, for which various diagnostic methods, including optical methods, have been developed. For the study of electrons, diagnostic methods are associated with the use of constant and alternating electric fields. In [3, 4], the process of electron evaporation was studied by means of constant electric field in the xenon UCP, that is, the escape of a part of the electrons from the plasma cloud.

Results were obtained for the fraction of remaining electrons as a function of the number of particles, density and the initial kinetic energy of the electrons. In [5], in addition to a constant field, a radio-frequency field with frequency of 5 to 40 MHz and with wavelength much larger than the plasma size was also used to study electrons in the UCP of xenon atoms. By means of scanning the frequency of the rf field within the said range at various times of the plasma expansion, the authors of [5] recorded the resonant signal of the electron output at a certain frequency. Authors of [6] observed in the xenon UCP collective modes which were excited by radio-frequency electric fields and were detected by means of enhanced electron emission during plasma expansion. In [2, 5–8], dependences of the resonant frequencies of electrons on the charge imbalance in the UCP were obtained. Analysis of the results of experiments by means of an rf electric field requires a study of natural oscillations of an inhomogeneous non-neutral plasma. The first studies of this kind [9–11] are devoted to bounded plasmas with cylindrical symmetry, where the electron component is confined by a strong magnetic field. A detailed description of these studies is given in the monograph [12]. Papers [13, 14] are devoted to the study of eigen-oscillations of a spherically symmetric bounded plasma, in which the electronic component is held by an electric field caused by a charge imbalance. As shown in [14], in the absence of friction, i.e. momentum transfer from the electronic component to the ion one, the spectrum of natural vibrations is continuous. In [13] individual discrete levels of plasma eigenoscillations were obtained. The interaction of plasma with an RF field was simulated by means of molecular dynamics. The simulation takes into account friction. The paucity of detected RF absorption resonances corresponding to discrete levels of natural oscillations does not allow one to describe the spectrum as a whole, its dependence on the imbalance and plasma density, which decreases with plasma expansion, as was observed in the experiment [6].

In this paper we use a method based on solving the known equation for the electric field. This takes into account the interaction of the field with the plasma by means of conductivity $\mu(\omega, \mathbf{r})$ and dielectric permittivity $\varepsilon(\omega, \mathbf{r})$ (ω is frequency of the rf electric field), which relate the local values of the current density and electric induction to the local value of the electric field intensity. Such statement of the problem limits the range of its applicability to conditions assuming that the mean free path of electron is small compared to the characteristic length of the field variation. The calculations were performed in relation to the experimental conditions [5–7]. The use of this method allowed us to

* bzelener@mail.ru

explain the dependence of the spectrum of natural oscillations of a spherical plasma on the charge imbalance and on the expansion time. At the same time, good agreement with experimental data was obtained [5–7].

II. CALCULATION MODEL

The calculations are performed for the experimental conditions of [5–7]. We consider the plasma that emerges upon single ionization of a limited volume of a cooled neutral gas (~ 1 mK). Characteristic initial dimensions of the plasma σ_0 in experiments are limited to fractions of a centimeter, the number of ions and electrons N_i , N_e are from 10^4 to 10^8 and the temperature T_e of electrons formed during the ionization is between one and few hundred degrees Kelvin. At the initial stages of the free expansion of the plasma over times of the order of σ_0/v_{T_e} (v_{T_e} is the thermal speed of electrons), that is, of the order of fractions of a microsecond, fast electrons leave the plasma. The resulting charge imbalance creates an electric field that prevents further leakage of electrons, therefore $\Delta N = N_i - N_e$ remains constant. In order to calculate ΔN , the results of [3, 15] are used. Plasma expansion takes place at a rate characteristic for the ion component, which are several orders of magnitude lower than that for the electron component. This makes it possible to consider the configuration of the ion component as quasi-stationary when studying [15] the motion of the electronic component of the plasma. In particular, in consideration of the motion of the electronic component, the current value of the plasma size $\sigma(t)$ ($\sigma(0) = \sigma_0$) is assumed to be constant. This said size is determined by the equality $\sigma_0(t) = \sqrt{\langle r^2/3 \rangle}$ where angular brackets denote averaging over the ionic configuration. We consider interaction of the electronic component with an electromagnetic field whose wavelength is much larger than the plasma size, which makes it possible to neglect the influence of the vector potential.

In the linear approximation for potential Φ , the electric field $\mathbf{E} = -\nabla\Phi\exp(i\omega t)$ arising under the action of an external field $\mathbf{E}_0 = \mathbf{k}E_0\cos(\omega t)$ (the field corresponds to the orbital number $l = 1$; \mathbf{k} is the unit vector along the z axis) is determined by the following equation:

$$\nabla(\varepsilon\nabla\Phi) = 0. \quad (1)$$

Here the permittivity is related to the conductivity μ as follows [16] :

$$\begin{aligned} \varepsilon &= 1 - \frac{4\pi i}{\omega}\mu = \varepsilon_1 + i\varepsilon_2 \\ \mu &= \mu_1 + i\mu_2 \sim n_e(r), \end{aligned} \quad (2)$$

where $n_e(r)$ is the electron density.

Setting $\Phi = (\varphi_1 + i\varphi_2)\exp(i\omega t)$ into equation (1), we obtain a system of second-order linear equations (A7) for the functions φ_1 and φ_2 , with two boundary conditions in the center and two at infinity (the complete derivation of the system of equations (A7) is presented in Appendix A):

$$\varphi_1(0) = \varphi_2(0) = 0 \text{ at } r = 0, \varphi_1 + E_0r \rightarrow 0, \varphi_2 \rightarrow 0 \text{ at } r \rightarrow \infty, \alpha = (\varepsilon_1\varepsilon'_1 + \varepsilon_2\varepsilon'_2)/(\varepsilon_1^2 + \varepsilon_2^2), \beta = (\varepsilon_2\varepsilon'_1 - \varepsilon_1\varepsilon'_2)/(\varepsilon_1^2 + \varepsilon_2^2).$$

In our calculations, the region where the electron concentration differs from zero is limited. At $r < x_0\sigma$, $n_e \sim \exp(-r^2/2\sigma^2)$; at $x_0\sigma < r < R = (x_0 + 1/x_0)\sigma$, concentration varies linearly from $n_e(x_0\sigma)$ to zero while remaining smooth at the point $x_0\sigma$. In our calculations, the region of nonzero electron density was limited. For $r < x_0\sigma$ $n_e \sim \exp(-r^2/2\sigma^2)$, and in the region $r > x_0\sigma$ the exponential profile was replaced by a tangent at the point $r = x_0\sigma$ until it intersected with the r axis at the point $R = (x_0 + 1/x_0)\sigma$. The fact that the concentration in the region $r > R$ is zero makes it possible to replace the boundary conditions at $r \rightarrow \infty$ by equivalent conditions at $r = R$:

$$\begin{aligned} 2\varphi_1 + r_0\varphi'_1 &= -3E_0 \\ 2\varphi_2 + r_0\varphi'_2 &= 0. \end{aligned} \quad (3)$$

The chosen scheme for numerical calculation of equations (A7) consists in selecting $\varphi'_1(0)$ and $\varphi'_2(0)$ which would fulfill the boundary conditions at $r = R$. With this calculation scheme, the admissible values of x_0 are determined by the accuracy of the computing device employed, since the accuracy of determining $\varphi'_1(0)$ and $\varphi'_2(0)$ is limited by the number of binary digits in the representation of numbers. In our case, the allowed values of x_0 should not exceed $x_0 = 3$.

Numerical solution of equations (A7) (Appendix A) makes it possible to determine the conditions for an increase of heat release in the plasma, which is accompanied in the experiment by an increase in the registered flux of electrons leaving the plasma region. The total heat release is given by the integral (B5) (see Appendix B). As the frequency of the external electric field approaches the frequency of natural oscillations, the heat release tends to infinity, which makes it possible to determine the spectrum of natural oscillations of the plasma under study.

III. ABSORPTION RESONANCES AT $\Delta N = 0$

First, let's consider the case of a small imbalance ($\Delta N = 0$), when the electric field generated by it can be neglected. In this case, the frequency dependence of conductivity and permittivity is given by the known relations [16]:

$$\begin{aligned}\mu &= \frac{e^2 n_e(r)}{m_e} \frac{\omega}{\omega\nu + i\omega^2} \\ \varepsilon &= 1 - \frac{\omega_p^2(r)}{\omega^2 - i\omega\nu},\end{aligned}\quad (4)$$

where ν is frequency of electron-ion collisions and $\omega_p(r) = \sqrt{4\pi e^2 n_e(r)/m_e}$. The value of ν is calculated by means of the formula for a weakly coupled plasma [17]:

$$\begin{aligned}\nu &= \frac{4\sqrt{2\pi}n_i e^2 \ln\Lambda}{3\sqrt{m_e}T_e^3} \\ \ln\Lambda &= \ln \frac{1}{\sqrt{3\Gamma_e^3}} \\ \Gamma_e &= \frac{e^2 \sqrt[3]{4\pi n_e/3}}{T_e},\end{aligned}\quad (5)$$

where T_e is equal to the average electron temperature in the plasma region and n_i is ionic concentration. The condition for the applicability of (4) is the smallness of the free path of electrons in comparison with the characteristic length of the electric field inhomogeneity d :

$$d \gg v_{T_e}/\nu, \quad (6)$$

where v_{T_e} is thermal electron velocity.

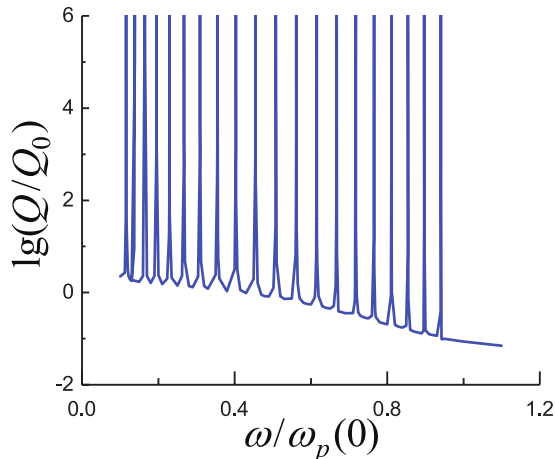


FIG. 1. Dependence logarithm of dimensionless Q/Q_0 on $\omega/\omega_p(0)$ at $\nu = 0.4\omega_p(0)$, $x_0 = 3$.

The solution of equations (A7) with boundary conditions (3) describe the plasma response to the effect of external RF radiation with a frequency of ω and an amplitude of E_0 . Figure 1 shows the dependence of heat release $Q/Q_0 = (4\pi\mu_1(0)E(0)^2)\sigma^3/3$ (see B5) on $\omega/\omega_p(0)$ at $\nu = 0.4\omega_p(0)$. Calculations demonstrate distinct heat release resonances, similar to Tonks-Dattner resonances. The same resonances of heat release were observed in calculations [13] performed by the method of molecular dynamics. When the resonant frequency $\tilde{\omega}$ is approached, the heat release grows inversely proportional to the square of the distance from the resonance $Q \sim 1/(\omega - \tilde{\omega})^2$, and functions φ_1 and φ_2 are inversely proportional to $\omega - \tilde{\omega}$.

The solutions of equations (A7) φ_1 and φ_2 also increase indefinitely inversely $\omega - \tilde{\omega}$, and the limits of the products $(\omega - \tilde{\omega})\varphi_{1,2}$ for $\omega \rightarrow \tilde{\omega}$ equal to $\tilde{\varphi}_{1,2}$ for are solutions of homogeneous equations (A7) (with $E_0 = 0$), that is, they represent the natural oscillations of the plasma formation under consideration. In fact, the lifetime of real oscillations

with a resonant frequency is limited by the condition of quasi-stationarity and does not exceed the interval Δt , within which the ion distribution can be considered unchanged. Accordingly, the width of the observed resonance cannot be less than $\Delta\omega = 2\pi/\Delta t$. The frequencies of such states form a discrete spectrum containing an apparently infinite number of frequencies in the region $\omega < \omega_p(0)$.

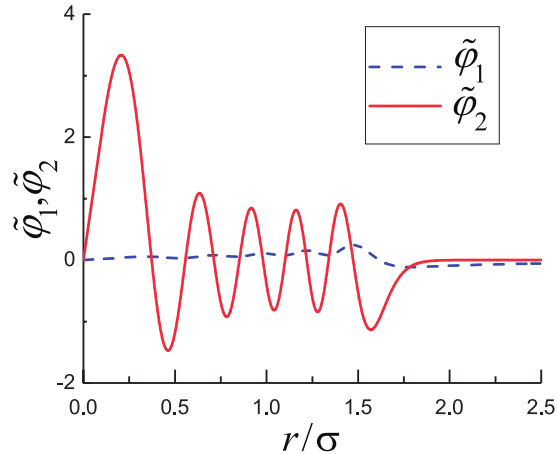


FIG. 2. Normalized eigensolutions of homogeneous equations (11) corresponding to the natural frequency $\omega/\omega_p(0) = 0.5077$ for $\omega_0 = 0$, $\nu = 0.4\omega_p(0)$, $x_0 = 3$ depending on r/σ : $\tilde{\varphi}_1$ is the blue curve, $\tilde{\varphi}_2$ is the red curve.

Figure 2 shows an example of a solutions of homogeneous equations (A7) normalized by means of the equality $\int(\varphi_1^2 + \varphi_2^2)r^2 dr/\sigma^3 = 1$ corresponding to the tenth resonance ($\tilde{\omega} = 0.5077\dots\omega_p(0)$). The blue curve corresponds to the function φ_1 , the red curve corresponds to the function φ_2 . The number of extrema of the function $\tilde{\varphi}_2$ is equal to the serial number N of resonances, numbered from right to left. Choosing σ/N as the characteristic size of the field inhomogeneity, we obtain from the inequality (5), which determines the range of applicability of the equations considered, the following estimate for the maximum number of natural frequencies:

$$N < \sigma v/v_{Te}. \quad (7)$$

With $\nu/\omega_p(0)$ decreasing, the distance between natural frequencies decreases. Figure 3 shows natural frequencies $\omega_n(\nu)$, numbered starting from the maximum frequency $\omega_1 \approx \omega_p$, for two values of the friction coefficient: $\nu/\omega_p(0) = 0.4$ is for the blue dash curve and $\nu/\omega_p(0) = 0.1$ is for the red solid curve.

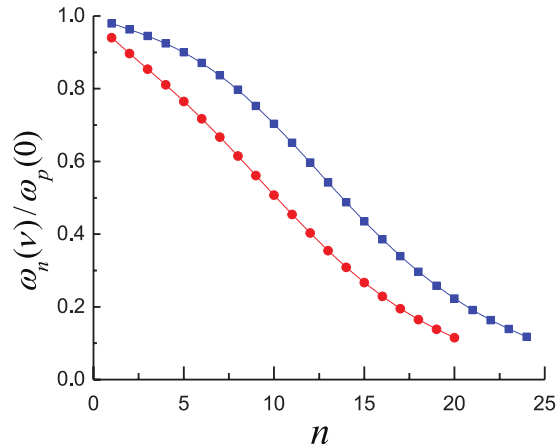


FIG. 3. Natural frequencies $\omega_n(\nu)/\omega_p(0)$, where n is the serial number of the resonance, for $\omega_0 = 0$ and for two values of the friction coefficient: $\nu/\omega_p(0) = 0.1$ corresponds to the blue curve and 0.4 corresponds to the red curve.

For small friction coefficients, the calculations are impossible due to the same reasons as for large values of x_0 . Calculations for $\nu/\omega_p(0)$ values greater than 0.1 show that the distance between resonant frequencies decreases with decreasing friction coefficient which agrees with the well-known fact that in the absence of friction the spectrum is continuous [14], similarly to the Trivelpiece-Gould spectrum [10].

IV. CALCULATION OF ABSORPTION RESONANCES WITH ACCOUNT TAKEN OF THE CHARGE IMBALANCE

In order to calculate the spectrum of natural oscillations of an inhomogeneous plasma, with account taken of the charge imbalance, it is necessary to determine the conductivity and dielectric permittivity of the plasma in the presence of a constant electric field. A similar problem was solved in [7] for the conditions where the electronic component is confined by means of a magnetic field. After a quasi-stationary mode for the electric field is established in the presence of spherical symmetry, the following self-similar expression is valid [15]:

$$\mathbf{E}(\mathbf{r}, t) = \frac{e\Delta N}{\sigma^3(t)} \mathbf{r} \eta \left(\frac{r}{\sigma(t)} \right), \quad (8)$$

where $\eta(\rho)$ is constant in the inner part of the plasma and, decreases proportionally to $1/\rho^3$ outside it. For the potential energy of electrons, we have:

$$\varphi = -\frac{e\Delta N}{\sigma^3(t)} \int_0^r r' \eta(r'/\sigma(t)) dr' \approx -\frac{e\Delta N}{\sigma^3(t)} \eta(0) \frac{r^2}{2} = \frac{m_e \omega_0^2(t)}{2} r^2. \quad (9)$$

With account taken of the following estimates: $\eta(0) \approx 1$; $\Delta N \approx \sqrt{kT_e N_i \sigma_0}/e$ [3, 15], we obtain:

$$\omega_0^2(t) \approx \frac{e\sqrt{kT_e N_i \sigma_0}}{m_e \sigma^3(t)}. \quad (10)$$

Let us represent the solution of the equation of motion of an individual electron in an external electric field $\mathbf{E} = \mathbf{E}(\mathbf{r}) \exp(i\omega t)$, with account taken of the friction coefficient ν :

$$m_e \ddot{\mathbf{r}} + m_e \mathbf{r} \omega_0^2 + m_e \nu \dot{\mathbf{r}} = -e \mathbf{E}(\mathbf{r}) e^{i\omega t} \quad (11)$$

in following form:

$$\mathbf{r}(t) = \mathbf{r}_0(t) + \Delta \mathbf{r}(t) \quad (12)$$

where $\mathbf{r}_0(t)$ is the solution of this equation for $\mathbf{E}(\mathbf{r}) = 0$ and

$$\Delta \mathbf{r}(t) = -\frac{e}{m_e \omega_1} \int_0^t e^{-\nu(t-t')/2} \sin(\omega_1(t-t')) \mathbf{E}(\mathbf{r}(t')) e^{i\omega t'} dt' \quad (13)$$

where $\omega_1^2 = \omega_0^2 - \nu^2/4$.

In the conditions where the mean free path of electron (v_{T_e} is the thermal velocity of electrons) is less than the characteristic size of the field variation d (inequality (6)), the following expression is valid for $\Delta \dot{\mathbf{r}}(t)$:

$$\begin{aligned} \Delta \dot{\mathbf{r}}(t) &\approx \frac{e}{m_e \omega_1} \mathbf{E}(\mathbf{r}(t)) e^{i\omega t} \\ &\cdot \int_0^\infty e^{-(\nu/2 + i\omega t)t} \cdot (\omega_1 \cos \omega_1 t - 0.5\nu \sin \omega_1 t) dt \\ &= -\frac{e\omega}{m_e} \mathbf{E}(\mathbf{r}(t)) e^{i\omega t} \frac{\omega}{\omega\nu - i(\omega_0^2 - \omega^2)}. \end{aligned} \quad (14)$$

For the electron current we have:

$$\mathbf{j}(\mathbf{r}) = \int f(\mathbf{r}(0), \dot{\mathbf{r}}(0)) \dot{\mathbf{r}}(t) d\mathbf{r}(0) d\dot{\mathbf{r}}(0), \quad (15)$$

where $f(\mathbf{r}(0), \dot{\mathbf{r}}(0))$ is the quasi-equilibrium electron distribution function $\int f(\mathbf{r}, \dot{\mathbf{r}}) d\dot{\mathbf{r}} = n_e(\mathbf{r})$, for which the following equality is valid within the linear approximation: $f(\mathbf{r}(0), \dot{\mathbf{r}}(0)) = f(\mathbf{r}(t), \dot{\mathbf{r}}(t))$.

After the following change of variables in (15): $\mathbf{r}(0), \dot{\mathbf{r}}(0) \rightarrow \mathbf{r}(t), \dot{\mathbf{r}}(t)$, we obtain for the current:

$$\begin{aligned} \mathbf{j}(\mathbf{r}) &= \mu(\mathbf{r}, \omega) \mathbf{E}(\mathbf{r}) e^{i\omega t} \\ \mu(\mathbf{r}, \omega) &= \frac{e^2 n_e(\mathbf{r})}{m_e} \frac{\omega}{\omega\nu - i(\omega_0^2 - \omega^2)} = \mu_1 + i\mu_2, \end{aligned} \quad (16)$$

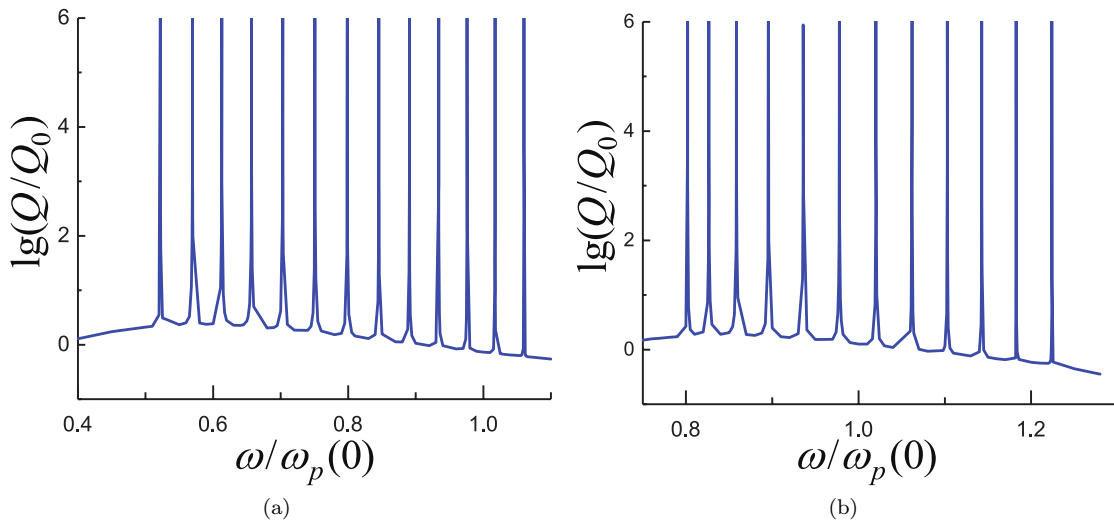


FIG. 4. Dependence of the logarithm of the dimensionless quantity Q/Q_0 on $\omega/\omega_p(0)$ at $\nu = 0.4\omega_p(0)$ $x_0 = 3$: (a) $\omega_0 = 0.5\omega_p(0)$; (b) $\omega_0 = 0.8\omega_p(0)$;

where μ is local plasma conductivity. For the dielectric permittivity we have:

$$\varepsilon = 1 - \frac{4\pi i}{\omega}(\mu_1 + i\mu_2) = 1 - \frac{\omega_p^2}{\omega^2 - \omega_0^2 - i\omega\nu} = \varepsilon_1 + i\varepsilon_2, \quad (17)$$

where $\omega_p = \sqrt{4\pi e^2 n_e(\mathbf{r})/m_e}$ is the plasma frequency.

Numerical solution of equations (A7) with dielectric permittivity (17) show that in the presence of friction, the spectrum remains discrete, but with a finite number of natural frequencies, limited by the minimal frequency $\sim \omega_0$. Figure 4 shows the dependence of heat release Q on $\omega/\omega_p(0)$ at $\nu = 0.4\omega_p(0)$ and $\omega_0 = 0.5\omega_p(0)$ (4(a)) and $\omega_0 = 0.8\omega_p(0)$ (4(b)) with all natural frequencies. The minimum of the resonant frequency is close to $\omega = \omega_0$. It follows from the above-said expression for the frequency ω_0 that its time dependence is determined by the following relation: $\omega_0 \sim \sqrt{\Delta N/\sigma(t)^3}$. A similar time dependence of the resonant frequency was observed in experiments [7]. In the stationary expansion mode, where ΔN and the plasma expansion velocity reach stationary values ($\sigma(t) \sim t$), the following relation is valid for time dependence of the frequency ω_0 : $\omega_0 \sim t^{-3/2}$.

V. COMPARISON WITH EXPERIMENT

Figure 5 shows the results of our calculation of the frequencies of the main resonances ω_0 on the basis of (9) in comparison with the experiment [5]. The ratio $\omega_0(t)/\omega_p(0, t)$ does not depend on time. The experimental values are obtained by means of digitizing Fig. 1 of [5]. Unfortunately, for other parameters of the xenon UCP, [5] does not provide resonance frequencies, but only gives the results of processing for the expansion time dependence of the average density.

Figure 6 shows the results of our calculations of the fundamental frequencies of electronic resonances ω_0 and the frequencies of the first three modes on the basis of (A7) with dielectric permittivity (17), in comparison with experiment [6]. The ratio $\omega_0(t)/\omega_p(0, t)$ in these conditions is 0.25 ($\sigma_0 = 0.028$ cm, $n_0 = 2 \cdot 10^9$ cm $^{-3}$, $T_e = 100$ K). The lower curve (the main resonance ω_0) is calculated by means of (17). The other three curves are obtained from the above-described calculations for the ratios of the next resonances to the main resonance ω_k/ω_0 . The curve following the first one corresponds to the 1st experimental resonance from [6], the next curve corresponds to the 2nd experimental resonance from [6], and the last curve corresponds to the 3rd experimental resonance from [6]. Agreement with experiments [5, 6] can be considered good.

In [7], the experimental dependence of $\omega_0/\omega_p(0)$ on the charge imbalance $\Delta N/N_i$ was obtained. However, it was obtained for different $\sigma(t)$ and there are no data in [7] concerning what particular UCP expansion time the imbalance values correspond to. It is stated in [7] that the results are average values of multi-data processing for $T_{e0} = 100$ K and for the range $N_i = (0.6 - 1) \cdot 10^6$ and $\sigma(t) = (0.04 - 0.06)$ cm.

We have calculated the experimental points for $T_{e0} = 100$ K, $N_i = 10^6$ and the imbalance values obtained in the experiment within the framework of (17) for the purposes of determining $\sigma(t)$. It turned out that $\sigma(t)$ in fact varies

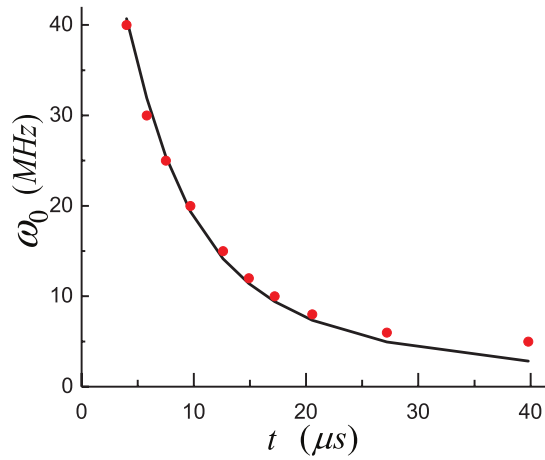


FIG. 5. Comparison of calculations with experiment [5]. Points are for the experiment, the curve is for the calculation (9). UCP parameters: $\sigma_0 = 0,022$ cm, $N_i = 8 \cdot 10^4$, $T_{e0} = 26$ K

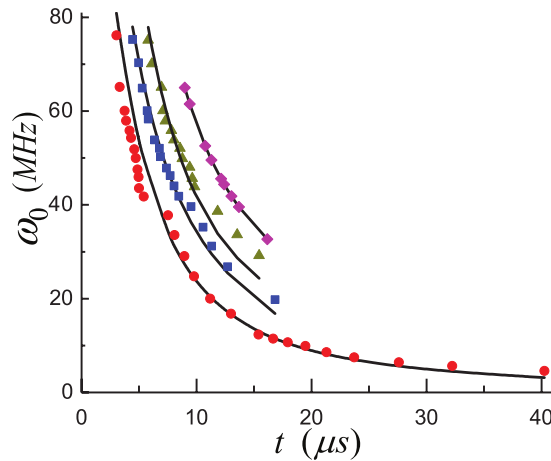


FIG. 6. Comparison of calculations with experiment [6]. Points are for the experiment, the lower curve is for calculation (17); the next curves are from numerical solution of (??) with dielectric permittivity (17). UCP parameters: $\sigma_0 = 0.028$ cm, $N_i = 1.5 \cdot 10^6$, $T_e = 100$ K, $\nu_{ei0} = 24$ MHz.

from 0.04 to 0.06 cm with the imbalance obtained in the experiment growing. Figure 7 shows the results of our calculations.

VI. CONCLUSION

In the present paper, the spectrum of natural oscillations of a spherical plasma is obtained as a function of charge imbalance. A method is used which is based on solving the well-known equations for electric field whose interaction with plasma is taken into account by means of dielectric permittivity $\epsilon(\omega, \mathbf{r})$ (where ω is frequency of the RF field). The range of applicability of this approach is limited by the conditions that assume that the mean free path of electrons is small compared to the characteristic length of the field variation. Good agreement with experiment is obtained.

VII. ACKNOWLEDGMENTS

The research was supported by the Russian Science Foundation Grant No. 21-72-00011 in the part of processing and analysis of the experiment and No. 23-72-10031 in the part of large-scale reworked this article within the framework of the new grant. This work was supported by the Ministry of Science and Higher Education of the Russian Federation

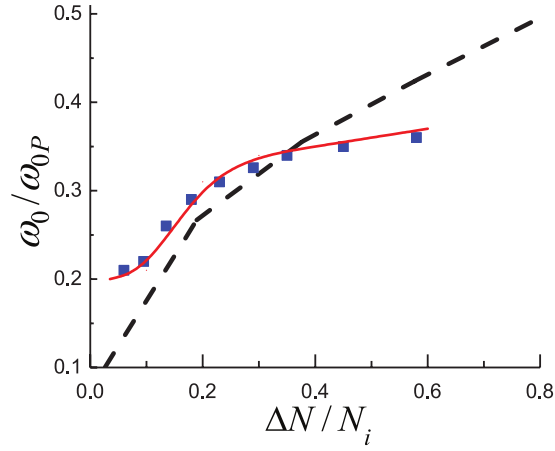


FIG. 7. Results of our calculations (the solid curve) in comparison with the experimental results [7] (points) and calculations [13] (the dotted line).

(State Assignment No. 075-01129-23-00) in the part of creating a program code for the numerical solution of a system of two second-order differential equations with complex boundary conditions. This research was also supported by computational resources of HPC facilities at HSE University.

Appendix A

Here is a description, omitted in the text, of the transition from equation (1) to a system of two real equations (A7) for φ_1 and φ_2

$$\text{Re} [\nabla \varepsilon \nabla \Phi e^{i\omega t}] = D_1 \cos(\omega t) + D_2 \sin(\omega t) = 0 \quad (\text{A1})$$

$$\begin{aligned} D_1 &= \varepsilon_1 \Delta \Phi_1 - \varepsilon_2 \Delta \Phi_2 + \nabla \varepsilon_1 \nabla \Phi_1 - \nabla \varepsilon_2 \nabla \Phi_2 = 0 \\ D_2 &= \varepsilon_1 \Delta \Phi_2 - \varepsilon_2 \Delta \Phi_1 + \nabla \varepsilon_1 \nabla \Phi_2 - \nabla \varepsilon_2 \nabla \Phi_1 = 0 \end{aligned} \quad (\text{A2})$$

$$\begin{aligned} \frac{1}{\varepsilon_1^2 + \varepsilon_2^2} (\varepsilon_1 D_1 + \varepsilon_2 D_2) &= \Delta \Phi_1 + \frac{\varepsilon_1 \nabla \varepsilon_1 + \varepsilon_2 \nabla \varepsilon_2}{\varepsilon_1^2 + \varepsilon_2^2} \nabla \Phi_1 + \frac{\varepsilon_2 \nabla \varepsilon_1 - \varepsilon_1 \nabla \varepsilon_2}{\varepsilon_1^2 + \varepsilon_2^2} \nabla \Phi_2 = 0 \\ -\frac{1}{\varepsilon_1^2 + \varepsilon_2^2} (\varepsilon_2 D_1 + \varepsilon_1 D_2) &= \Delta \Phi_2 + \frac{\varepsilon_1 \nabla \varepsilon_1 + \varepsilon_2 \nabla \varepsilon_2}{\varepsilon_1^2 + \varepsilon_2^2} \nabla \Phi_2 + \frac{\varepsilon_2 \nabla \varepsilon_1 - \varepsilon_1 \nabla \varepsilon_2}{\varepsilon_1^2 + \varepsilon_2^2} \nabla \Phi_1 = 0 \end{aligned} \quad (\text{A3})$$

$$\begin{aligned} \frac{\varepsilon_1 \nabla \varepsilon_1 + \varepsilon_2 \nabla \varepsilon_2}{\varepsilon_1^2 + \varepsilon_2^2} &= \alpha \frac{\mathbf{r}}{r} \\ \frac{\varepsilon_2 \nabla \varepsilon_1 - \varepsilon_1 \nabla \varepsilon_2}{\varepsilon_1^2 + \varepsilon_2^2} &= \beta \frac{\mathbf{r}}{r} \end{aligned} \quad (\text{A4})$$

$$\begin{aligned} \alpha &= \frac{\varepsilon_1 \varepsilon_1' + \varepsilon_2 \varepsilon_2'}{\varepsilon_1^2 + \varepsilon_2^2} \\ \beta &= \frac{\varepsilon_2 \varepsilon_1' - \varepsilon_1 \varepsilon_2'}{\varepsilon_1^2 + \varepsilon_2^2} \end{aligned} \quad (\text{A5})$$

$$\begin{aligned} \frac{\mathbf{r}}{r} \nabla \Phi_\alpha &= \phi_\alpha' \cos(\theta) \\ \nabla \Phi_\alpha &= \left(\frac{1}{r^2} \frac{d}{dr} \left(r^2 \frac{d\varphi_\alpha}{dr} \right) - \frac{2}{r^2} \varphi_\alpha \right) \cos(\theta) \end{aligned} \quad (\text{A6})$$

$$\begin{aligned}
\frac{1}{r^2} \frac{d}{dr} \left(r^2 \frac{d\varphi_1}{dr} \right) - \frac{2}{r^2} \varphi_1 + \alpha \frac{d\varphi_1}{dr} + \beta \frac{d\varphi_2}{dr} &= 0 \\
\frac{1}{r^2} \frac{d}{dr} \left(r^2 \frac{d\varphi_2}{dr} \right) - \frac{2}{r^2} \varphi_2 + \alpha \frac{d\varphi_2}{dr} - \beta \frac{d\varphi_1}{dr} &= 0
\end{aligned} \tag{A7}$$

Appendix B

Derivation of the expression for for total heat release (brackets indicate time averaging) $Q = \int dr \langle q \rangle$:

$$\begin{aligned}
q &= \text{Re} \mathbf{E} \text{Re} \mathbf{J} = \text{Re} \mathbf{E} \text{Re} (\mu_1 + i\mu_2) \mathbf{E} \\
&= (\mu_1 (\nabla \Phi_1 \cos(\omega t) - \nabla \Phi_2 \sin(\omega t)) - \mu_1 (\nabla \Phi_1 \sin(\omega t) - \nabla \Phi_2 \cos(\omega t))) \cdot \\
&\quad \cdot (\nabla \Phi_1 \cos(\omega t) - \nabla \Phi_2 \sin(\omega t)) = \\
\mu_1 ((\nabla \Phi_1)^2 \cos(\omega t) - (\nabla \Phi_2)^2 \sin(\omega t)) - \mu_2 &\left[((\nabla \Phi_1)^2 - (\nabla \Phi_2)^2) \frac{\sin(2\omega t)}{2} \nabla \Phi_1 \Phi_2 \cos(2\omega t) \right] - \\
&\quad - \mu_1 \nabla \Phi_1 \Phi_2 \frac{\sin(2\omega t)}{2}
\end{aligned} \tag{B1}$$

$$\begin{aligned}
\langle \cos^2(\omega t) \rangle &= \langle \sin^2(\omega t) \rangle = \frac{1}{2} \langle \cos(2\omega t) \rangle = \langle \sin(2\omega t) \rangle = 0 \\
\langle q \rangle &= \frac{\mu_1}{2} ((\nabla \Phi_1)^2 + (\nabla \Phi_2)^2)
\end{aligned} \tag{B2}$$

$$\begin{aligned}
(\nabla \Phi_\alpha)^2 &= \frac{\varphi_\alpha^2}{r^2} + \cos^2 \theta \left(\varphi_\alpha'^2 + \frac{\varphi_\alpha^2}{r^2} - \frac{\varphi_\alpha \varphi_\alpha'}{r} \right) + 2 \cos^2 \theta \varphi_\alpha \left(\frac{\varphi_\alpha'}{r} - \frac{\varphi_\alpha}{r^2} \right) = \\
&\quad \sin^2 \theta \frac{\varphi_\alpha^2}{r^2} + \cos^2 \theta \varphi_\alpha'^2
\end{aligned} \tag{B3}$$

$$\langle q \rangle = \frac{\mu_1}{2} \left(\sin^2 \theta \frac{\varphi_2^2}{r^2} + \varphi_2'^2 + \cos^2 \theta (\varphi_1'^2 + \varphi_2'^2) \right) \tag{B4}$$

$$Q = \int dr \langle q \rangle = \frac{2\pi}{3} \int_0^{r_0} \mu_1 \left(\varphi_1^2 + \varphi_2^2 + 2 \cdot r^2 \left\{ \left(\frac{d\varphi_1}{dr} \right)^2 + \left(\frac{d\varphi_2}{dr} \right)^2 \right\} \right) dr. \tag{B5}$$

-
- [1] Thomas C Killian, T Pattard, T Pohl, and JM Rost. Ultracold neutral plasmas. *Physics Reports*, 449(4-5):77–130, 2007.
 - [2] M Lyon and SL Rolston. Ultracold neutral plasmas. *Reports on Progress in Physics*, 80(1):017001, 2016.
 - [3] TC Killian, S Kulin, SD Bergeson, Luis A Orozco, C Orzel, and SL Rolston. Creation of an ultracold neutral plasma. *Physical Review Letters*, 83(23):4776, 1999.
 - [4] KA Twedt and SL Rolston. Electron evaporation from an ultracold plasma in a uniform electric field. *Physics of Plasmas*, 17(8):082101, 2010.
 - [5] S Kulin, TC Killian, SD Bergeson, and SL Rolston. Plasma oscillations and expansion of an ultracold neutral plasma. *Physical review letters*, 85(2):318, 2000.
 - [6] RS Fletcher, XL Zhang, and SL Rolston. Observation of collective modes of ultracold plasmas. *Physical review letters*, 96(10):105003, 2006.
 - [7] KA Twedt and SL Rolston. Electronic detection of collective modes of an ultracold plasma. *Physical Review Letters*, 108(6):065003, 2012.
 - [8] Truman M Wilson, Wei-Ting Chen, and Jacob L Roberts. Density-dependent response of an ultracold plasma to few-cycle radio-frequency pulses. *Physical Review A*, 87(1):013410, 2013.
 - [9] AW Trivelpiece and RW Gould. Space charge waves in cylindrical plasma columns. *Journal of Applied Physics*, 30(11):1784–1793, 1959.

- [10] Adam Dattner. Resonance densities in a cylindrical plasma column. *Physical Review Letters*, 10(6):205, 1963.
- [11] M Gagneaux and PE Vandenplas. Temperature (tonks–dattner) resonances theoretically revisited: New temperature and density diagnostics. *The Physics of fluids*, 29(5):1472–1479, 1986.
- [12] Ronald C Davidson. *Physics of nonneutral plasmas*. World Scientific Publishing Company, 2001.
- [13] Andrei Lyubonko, Thomas Pohl, and Jan-Michael Rost. Energy absorption of quasineutral plasmas through electronic edge-modes. *arXiv preprint arXiv:1011.5937*, 2010.
- [14] Scott D Bergeson and Ross L Spencer. Neutral-plasma oscillations at zero temperature. *Physical Review E*, 67(2):026414, 2003.
- [15] EV Vikhrov, S Ya Bronin, BB Zelener, and BV Zelener. Ion wave formation during ultracold plasma expansion. *Physical Review E*, 104(1):015212, 2021.
- [16] LD Landau and EM Lifshitz. *Electrodynamics of Continuous Media*. FizMatLit, 1959.
- [17] Lyman Spitzer. *Physics of fully ionized gases*. Courier Corporation, 2006.

